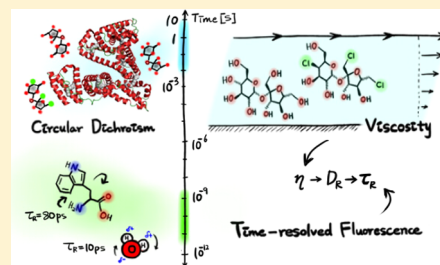


Sucralose Destabilization of Protein Structure

Lee Chen,[†] Nimesh Shukla,[†] Inha Cho,[†] Erin Cohn,[‡] Erika A. Taylor,[‡] and Christina M. Othon*,[†][†]Department of Physics, Wesleyan University, 265 Church Street, Middletown, Connecticut 06459, United States[‡]Department of Chemistry, Wesleyan University, 52 Lawn Avenue, Middletown, Connecticut 06459, United States

S Supporting Information

ABSTRACT: Sucralose is a commonly employed artificial sweetener that behaves very differently than its natural disaccharide counterpart, sucrose, in terms of its interaction with biomolecules. The presence of sucralose in solution is found to destabilize the native structure of two model protein systems: the globular protein bovine serum albumin and an enzyme staphylococcal nuclease. The melting temperature of these proteins decreases as a linear function of sucralose concentration. We correlate this destabilization to the increased polarity of the molecule. The strongly polar nature is manifested as a large dielectric friction exerted on the excited-state rotational diffusion of tryptophan using time-resolved fluorescence anisotropy. Tryptophan exhibits rotational diffusion proportional to the measured bulk viscosity for sucrose solutions over a wide range of concentrations, consistent with a Stokes–Einstein model. For sucralose solutions, however, the diffusion is dependent on the concentration, strongly diverging from the viscosity predictions, and results in heterogeneous rotational diffusion.



Small molecular osmolytes are used in nature to regulate the stability of solvated protein structures. Disaccharides such as trehalose and sucrose have attracted much attention because they appear unique in protecting biological organisms from diverse physical stresses including cryogenic storage,^{1,2} elevated temperature,^{3,4} dehydration,⁵ and excess salinity.⁶ This property has led to the widespread use of disaccharides in the cosmetic, food, and pharmaceutical industries. Although the efficacies of disaccharides in biopreservation are well-established, the molecular mechanisms that stabilize cellular structure and function are less clear.⁷ The biopreservation properties of disaccharide osmolytes are often attributed to their water-structuring capabilities.^{8,9} To explore the chemical and structure–function relationship of disaccharides more thoroughly, we chose to investigate the stability of model protein systems in the presence of both sucrose and the unnatural sugar replacement, sucralose.

Very little has been reported about the interaction of sucralose with biomolecules; however, concern is rising over its accumulation in the natural environment as its synthetic nature ensures it is not readily metabolized.^{10–17} It is widely believed that because of its low bioavailability any presence in the environment would have minimal impact; however, as has been recently shown for animal studies,^{14,17,18} and as we demonstrate in this work, sucralose can interact strongly with biomolecules. We compare its physical interactions with those of the natural disaccharide sucrose. The structure of each molecule is displayed in Scheme 1.

We chose two well-characterized model protein systems to investigate the impact of protein structural stability. Bovine serum albumin (BSA) is well-established as a model protein for structural investigations due to its low cost, abundance, well-established structural characterization, homology with the

human serum albumin, and its well-known binding properties.¹⁹ BSA is a highly helical globular protein system that exhibits a stable native structure at room temperature in solutions near physiological pH and salt concentrations. Staphylococcal nuclease (SN) is an endonuclease that preferentially digests single-stranded nucleic acids, which is easily expressed at high purity from *E. coli*.^{20,21} SN exhibits a far more flexible structure, which includes both helical and β -sheet domains.²² By comparing the stability of these two systems in the presence of our disaccharide and artificial sweetener, we can generalize the interaction to be nonsequence specific.

Circular dichroism (CD) spectroscopy was used to determine the melting temperature of the proteins in the presence of increasing disaccharide or artificial sweetener concentration. Our results indicate that the protein structures are destabilized with increasing sucralose concentration. To further isolate the physical origin of this effect, we employed time-resolved and steady-state fluorescence spectroscopy using the probe biomolecule, tryptophan. On the basis of these biophysical assessments, we attribute the protein destabilization observed to strong electrostatic interactions arising from the highly polar nature of sucralose. These strong interactions can have important implications for the bioavailability and fate of such molecules in natural systems.

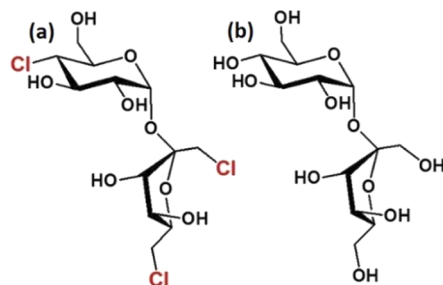
Thermal Unfolding of Protein Samples. The CD spectra of BSA and SN samples at low temperatures (5 to 25 °C) show a high helical content consistent with their native structures. Thermal denaturation curves are shown for BSA (panel a) and SN (panel c) in the absence of any disaccharide (Figure 1). The

Received: March 2, 2015

Accepted: March 26, 2015

Published: March 26, 2015

Scheme 1. (a) Sucralose and (b) Sucrose



characteristic double minima at 208 and 222 nm exhibited by helical proteins are observed at low temperatures and are reduced as temperature is elevated. Monitoring the ellipticity observed at 222 nm reveals structural unfolding for both BSA (panel b) and SN (panel d). Because of the high stability of the BSA globular structure, complete melting could not be obtained; therefore, for the purpose of fitting, the fully denatured ellipticity is set using the CD spectra from acid-denatured BSA at pH 1.7.

The melting temperature was determined from the inflection point arising from sigmoidal fitting of the ellipticity at 222 nm as a function of the temperature. The melting temperatures as a function of sugar and sweetener concentration are shown in Figure 2. Sucrose demonstrates a slight increase in melting temperature with concentration, consistent with its characterization as a naturally occurring kosmotrope.²³ In contrast, sucralose strongly decreases the melting temperature as a function of concentration. Even at room temperature, the

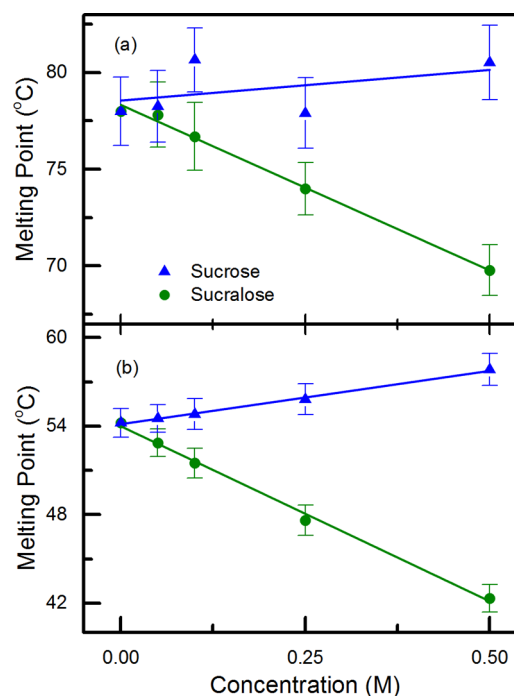


Figure 2. Melting temperature as a function of increasing sucrose (blue triangles) and sucralose (green circles) concentration for BSA (a) and SN (b).

structure exhibits a linear decrease in ellipticity, indicating that sucralose is destabilizing the native structure of both proteins. To further explore the physical origin of this effect, we

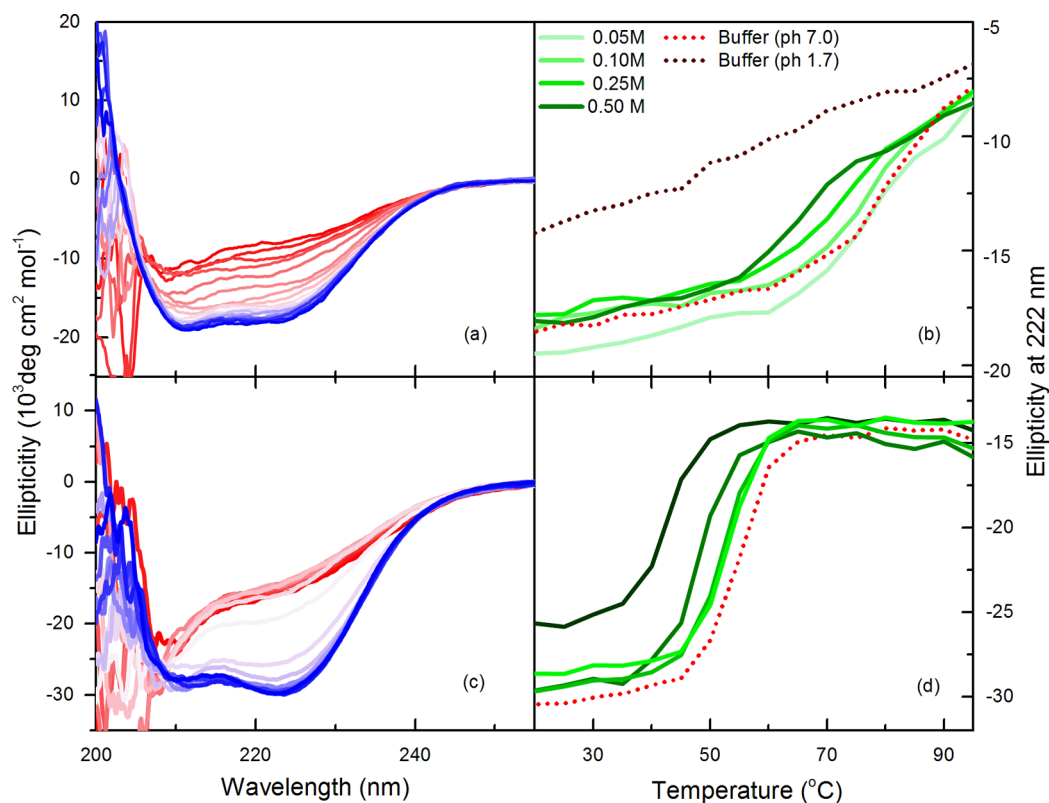


Figure 1. Circular dichroism spectra of BSA (a) and SN (c) in buffer as a function of increasing temperature from 5 to 95 °C. The melting temperature is determined by the inflection of the ellipticity at 222 nm versus temperature curves for BSA (b) and SD (d). Samples of increasing cosolute concentration (solid) as well as reference buffer curves (dotted) are shown.

Table 1. Rotational Correlation Times Obtained from Time-Resolved Anisotropy (τ), Stretch Exponential Fitting Parameter (β), and Measured Viscosity (η) for Sucrose and Sucralose Solutions

concentration (M)	sucrose			sucralose		
	τ (ps)	β_{stretch}	η (mPa·s)	τ (ps)	β_{stretch}	η (mPa·s)
0.010	79 ± 12	0.97 ± 0.06	1.03 ± 0.01	86 ± 16	0.73 ± 0.19	1.04 ± 0.01
0.025	74 ± 8.0	0.97 ± 0.04	1.06 ± 0.04	102 ± 27	0.66 ± 0.08	1.06 ± 0.02
0.050	88 ± 14	0.96 ± 0.08	1.07 ± 0.03	121 ± 26	0.67 ± 0.06	1.11 ± 0.04
0.075	85 ± 18	0.94 ± 0.06	1.11 ± 0.03	141 ± 29	0.66 ± 0.19	1.14 ± 0.03
0.100	90 ± 25	0.97 ± 0.06	1.15 ± 0.03	150 ± 39	0.74 ± 0.12	1.18 ± 0.04
0.250	114 ± 24	0.98 ± 0.04	1.26 ± 0.03	227 ± 20	0.53 ± 0.09	1.31 ± 0.04
0.500	112 ± 18	0.81 ± 0.17	1.65 ± 0.07	299 ± 58	0.61 ± 0.01	1.75 ± 0.05
0.750	139 ± 12	0.75 ± 0.13	2.11 ± 0.04	N/A	N/A	N/A
1.000	198 ± 16	0.77 ± 0.10	3.00 ± 0.22	N/A	N/A	N/A

considered the chemical and physical differences between the two molecules. The halogenation of sucrose alters the electrostatic dipole moment from approximately 2.8 to 4.6 D (calculated using density function theory and B3LYP; standard basis sets from 6 to 311G++ were used) and alters the hydrogen bonding capacity of the molecule. We have previously observed the change in hydration around halogenated biomolecules.²⁴

To investigate how these changes may alter bimolecular interactions, we measured the concentration-dependent interaction with the intrinsically fluorescent biomolecule, tryptophan. We measured steady-state absorption and fluorescence emission spectra for sucrose and sucralose solutions containing 3 mM of tryptophan. No change in the spectra, the total Stokes shift, or the lifetime of tryptophan was observable for any cosolute concentration. The lack of any spectral shift in the presence of either sucrose or sucralose indicates that there is no direct interaction between the sweeteners and the probe molecule. This is consistent with sucrose's role as a nonspecific osmolyte that only stabilizes proteins through solvent-mediated, indirect interaction.²³ For sucralose, this implies that any interaction between the probe and the cosolute must occur during the nonequilibrium interactions introduced by the excited state of the probe. The lack of apparent changes in either the absorption or emission spectra suggests that with the interactions are transient and sucralose is not directly interacting with tryptophan.

Further studies on the long-range interactions were probed using time-resolved techniques. The rotational diffusion of a fluorescent molecule (tryptophan) in solution with and without disaccharide was measured by time-resolved anisotropy and compared with the predicted correlation times given by a Stokes–Einstein–Debye (SED) rotational diffusion model. The SED model predicts the rotational diffusion of a spherical molecule will be proportional to the viscosity of the medium according to

$$D = \frac{k_B T}{8\pi\eta r^3} = \frac{1}{2\tau_R}$$

where η is the viscosity of the fluid and r is the radius of the molecule.²⁵ This model has been verified for a wide range of probe molecules and solvents. Corrections for the shape of the molecule can be introduced to improve the accuracy of such predictions.

We fit the rotational correlation decays with a stretched exponential model as the dynamics for sucralose concentration appear heterogeneous at all concentrations and cannot be fit

with a single exponential model. Values for the fits are given in Table 1. The rotational correlation time as a function of increasing solution viscosity (η) is shown in Figure 3. Included in this plot is the predicted diffusion time from a SED model based on the measured viscosity of the samples. The rotational correlation was measured at the same temperature, T , at which the viscosity was measured. For sucrose we note a fair agreement with prediction for the entire range of concentrations.

For sucralose samples the rotational diffusion of tryptophan strongly deviates from a SED diffusional model at all concentrations, although the measured viscosity of the sample remains virtually indistinguishable from sucrose solutions at the same concentrations. We interpret this divergence as the influence of the long-range dipolar interaction of sucralose molecules in solution with the excited state of tryptophan because the only observable difference between sucralose and sucrose occurs during the nonequilibrium transient state immediately after excitation. The dipole moment of sucrose (at 3.1 D)²⁶ does not appear to influence the rotational diffusion of tryptophan apart from the increase in bulk viscosity. Sucralose has a dipole moment that we calculate to be ~ 2.5 times that of water (at 4.6 D), and the electrostatic interactions

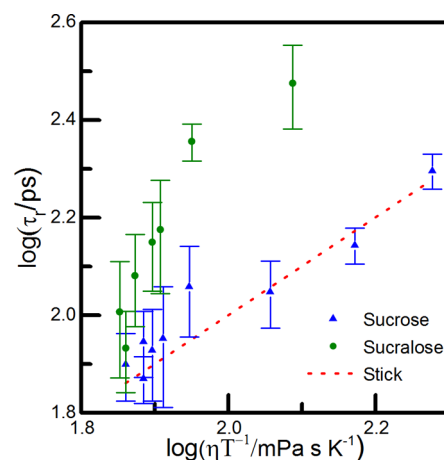


Figure 3. Rotation correlation time as measured by TCSPC for sucrose (blue triangles) and sucralose (green circles). Measurements of the viscosity of these solutions over the range explored were virtually indistinguishable. A prediction of the expected correlation time for the SED diffusional model is shown for stick conditions (dotted line).

between the probe molecule and the cosolute appear to become significant.

The presence of such long-range electrostatic interactions also explains the necessity for a stretched-exponential model in fitting the rotational correlation relaxation. The rotational diffusion of a tryptophan molecule will be slowed by electrostatic drag by the nearest neighbor cosolute interactions. The heterogeneity reflects the random distribution of sucralose around tryptophan in the ground state, which is further verification that no direct interaction between this specific probe and the cosolute exists in the equilibrium state. This random arrangement creates a distribution of nearest-neighbor distances between solute and cosolute; therefore, because dipolar interactions drop off as $1/r^6$, the force exerted on individual tryptophan molecules is inhomogeneous and the observed relaxation times are heterogeneous. This observation adds to the increasing number of ionic and polar systems exhibiting diffusion, which is inconsistent with a simple SED diffusional model.^{27–31}

The large electrostatic drag results in a rotational diffusion of the probe molecule that is strongly dependent on sucralose concentration. This results in a fractional diffusion dependence that is commonly observed for systems exhibiting heterogeneous diffusion.³² This form of strong electrostatic interaction may be responsible for the destabilization of the native structure observed and reduction of the melting temperature. The sucralose is likely interacting with polar and charged portions of the protein structure in a manner consistent with known chemical denaturants such as urea. Whereas sucralose only interacts with our probe molecule in its transient excited state, it is anticipated that sucralose would interact strongly with the permanent dipole moments of polar residues as well as the charged amino acids and possibly the protein backbone. It is interesting to note that urea that is known to destabilize protein structures via electrostatic interactions³³ also has a dipole moment of ~ 4.5 D, similar to the value we calculate for sucralose. This behavior is in direct contrast with the biopreservation properties of sucrose that does not exhibit strong electrostatic interactions. These biophysical studies of sucralose reveal strong biological interactions, the consequences of which are important to consider in the context of bioavailability and its interaction with bio-organisms.

■ EXPERIMENTAL DETAILS

Sample Preparation. Bovine serum albumin (98% purity) and sucralose (98%) were purchased from Sigma-Aldrich, tryptophan (99%) from Acros Organics, and sucrose (99%) from Alfa Aesar and were used without further purification. A 0.05 M NaH_2PO_4 buffer solution with pH 6.8 was prepared using ultrapure water. BSA concentration of 1 μM was prepared with various concentrations of disaccharides ranging from 0 to 1 M for sucrose and 0 to 0.50 M sucralose (very close to the solubility limit for sucralose). Samples were stored at <4 °C prior to use. SN was expressed and purified using the method described by Shortle and Meeker³⁴ with modifications outlined by Byrne et al.³⁵ Protein concentration was determined to be 23.0 mg/mL using the extinction coefficient $\epsilon_{280} = 0.93$ mg/mL $\cdot\text{cm}^2$.³⁴ SN samples were stored at -80 °C in water and thawed and adjusted to final concentration 1 mg/mL just prior to melting temperature measurements.

Circular Dichroism. The CD melting measurements are conducted on a Jasco spectropolarimeter (model J-810, Jasco International, Tokyo, Japan). A 2 mm path-length quartz

cuvette was used for all CD measurements. Thermal denaturation was measured from 5 to 95 °C, taking CD scans at 5° intervals. The data were taken in triplicate with each experiment containing three identical solutions and one reference buffer containing the same concentration of sugar. The buffer spectra are then subtracted from the sample spectra at each temperature. The melting temperature of the protein is determined by fitting a sigmoidal curve to the ellipticity at 222 nm using Microcal Origin 8. The final melting temperature is defined as the point of inflection in the fitting.

Time-Resolved Fluorescence Anisotropy. Steady-state fluorescence and UV–visible absorption spectroscopy are measured for all sugar concentrations. UV–visible absorption spectroscopy was measured on a PerkinElmer spectrophotometer. Steady-state fluorescence was measured on a Spex Fluoromax fluorometer using excitation at 295 nm with a 5 nm bandwidth. No change in the spectra, the total Stokes shift, or the lifetime of tryptophan was observable for any cosolute concentration. (See Figure S1 in the Supporting Information.) An example spectrum for 0.1 M is given in the Supporting Information.

Time-Resolved Fluorescence Spectroscopy. Excitation of tryptophan at 295 nm, for time-resolved measurements, was accomplished using the tripled output of a tunable Ti-sapphire oscillator (Coherent Chameleon Ultra II, pulse length 140 fs). The repetition rate was decreased to 10.6 MHz using a Conoptics pulse selector. The light was attenuated to 1.5 mW before illuminating a 1 cm path length cuvette. The temperature of the cuvette is maintained at 23 °C via a circulating water bath and monitored using a thermocouple probe. Light was collected at a right-angle geometry. The signal is detected at 410 nm and passed through a precision linear polarizer (BK 7 material, $\lambda/10$ flat), focused on to the input slit of a Jerrell Ash (82-410) monochromator and onto a single-photon avalanche photodiode (id100 ID Quantique). Signal output from the avalanche photodiode and a synchronization signal were fed into a time-correlated single photon counting (TCSPC) module (Becker-Hickl SPC-130 TCSPC). The system resolution was characterized by measuring the fwhm of the Raman scattering of water. Fluorescence lifetime is detected at the magic angle at wavelengths across the fluorescence spectrum (data not shown). The lifetime is determined by global fitting analysis and was found to be identical for sucrose and sucralose solutions and to be consistent with values found for tryptophan in the literature.

The rotational diffusion and mobility of the fluorescent probe is monitored by calculating the anisotropy

$$r(t) = \frac{I_{\parallel}(t) - GI_{\perp}(t)}{I_{\parallel}(t) + 2GI_{\perp}(t)}$$

where I_{\parallel} is the signal intensity with polarization parallel to the excitation polarization, I_{\perp} is the signal intensity with polarization perpendicular to the excitation polarization direction, and G represents the correction factor for the detector and monochromator sensitivity to different polarization orientations. The G factor for the system was determined experimentally by the tail matching method. Time-resolved anisotropy decay represents the rate of reorientation of the excitation dipole moment with respect to the excitation polarization vector, assuming the angle between the excitation absorption dipole and the emission dipole moment is approximately zero. An example rotational correlation curve is given in the Supporting Information Figure S2.

Viscosity Measurements. Viscosity of the tryptophan–disaccharide samples were measured using a Brookfield DV-2+ Pro viscometer with a cylindrical spindle (LV1) at 60 rpm. An 80 mL freeze-dry flask was used as a container for all measurements. The temperature of the room and solutions was maintained at 23.5 ± 0.5 °C. The spindle was given at least 2 min before reaching equilibrium in the solution before viscosity readings were taken. The viscosity pure water was measured as a reference point, and all other measurement values were normalized according to this value. For each species and concentration, four independent measurements were conducted. The measured viscosity of sucrose buffer solutions was found to be consistent with the reported viscosity of sucrose aqueous solutions.³⁶ The difference between sucrose and sucralose viscosity was small yet detectable and found to be within 7% of each other at all concentrations. The measured viscosity was then used to predict the rotational tumbling time of tryptophan in various disaccharide concentrations using the SED rotational diffusion model.

■ ASSOCIATED CONTENT

● Supporting Information

Steady-state absorption and emission spectrum and time-resolved fluorescence anisotropy. This material is available free of charge via the Internet at <http://pubs.acs.org>.

■ AUTHOR INFORMATION

Corresponding Author

*E-mail: cothon@wesleyan.edu.

Notes

The authors declare no competing financial interest.

■ ACKNOWLEDGMENTS

We thank Dr. Bertrand Garcia-Moreno E. (Johns Hopkins Department of Biophysics, Baltimore, MD) for generously providing the wild-type staphylococcal nuclease construct transformed into BL21(DE3) cells. This work has been supported by the Connecticut Space Grant Consortium.

■ REFERENCES

- (1) Somme, L.; Meier, T. Cold Tolerance in Tardigrada from Dronning-Maud-Land, Antarctica. *Polar Biol.* **1995**, *15*, 221–224.
- (2) Storey, K. B.; Storey, J. M. Frozen and Alive. *Sci. Am.* **1990**, *263*, 92–97.
- (3) Benaroudj, N.; Lee, D. H.; Goldberg, A. L. Trehalose Accumulation During Cellular Stress Protects Cells and Cellular Proteins from Damage by Oxygen Radicals. *J. Biol. Chem.* **2001**, *276*, 24261–24267.
- (4) Sola-Penna, M.; Meyer-Fernandes, J. R. Stabilization against Thermal Inactivation Promoted by Sugars on Enzyme Structure and Function: Why Is Trehalose More Effective Than Other Sugars? *Arch. Biochem. Biophys.* **1998**, *360*, 10–14.
- (5) Crowe, J. H. Anhydrobiosis - Unsolved Problem. *Am. Nat.* **1971**, *105*, 563–573.
- (6) Wright, J. C.; Westh, P.; Ramlov, H. Cryptobiosis in Tardigrada. *Biol. Rev. Cambridge Philos. Soc.* **1992**, *67*, 1–29.
- (7) Kent, B.; Hunt, T.; Darwish, T. A.; Hauss, T.; Garvey, C. J.; Bryant, G. Localization of Trehalose in Partially Hydrated Dopc Bilayers: Insights into Cryoprotective Mechanisms. *J. R. Soc., Interface* **2014**, *11*, 20140069.
- (8) Choi, Y.; Cho, K. W.; Jeong, K.; Jung, S. Molecular Dynamics Simulations of Trehalose as a 'Dynamic Reducer' for Solvent Water Molecules in the Hydration Shell. *Carbohydr. Res.* **2006**, *341*, 1020–1028.
- (9) Jain, N. K.; Roy, I. Effect of Trehalose on Protein Structure. *Protein Sci.* **2009**, *18*, 24–36.
- (10) Lange, F. T.; Scheurer, M.; Brauch, H. J. Artificial Sweeteners—a Recently Recognized Class of Emerging Environmental Contaminants: A Review. *Anal. Bioanal. Chem.* **2012**, *403*, 2503–2518.
- (11) Mawhinney, D. B.; Young, R. B.; Vanderford, B. J.; Borch, T.; Snyder, S. A. Artificial Sweetener Sucralose in U.S. Drinking Water Systems. *Environ. Sci. Technol.* **2011**, *45*, 8716–8722.
- (12) Mead, R. N.; Morgan, J. B.; Avery, G. B.; Kieber, R. J.; Kirk, A. M.; Skrabal, S. A.; Willey, J. D. Occurrence of the Artificial Sweetener Sucralose in Coastal and Marine Waters of the United States. *Mar. Chem.* **2009**, *116*, 13–17.
- (13) Tollefsen, K. E.; Nizzetto, L.; Huggett, D. B. Presence, Fate and Effects of the Intense Sweetener Sucralose in the Aquatic Environment. *Sci. Total Environ.* **2012**, *438*, 510–516.
- (14) Wiklund, A. K. E.; Adolfsson-Erici, M.; Liewenborg, B.; Gorokhova, E. Sucralose Induces Biochemical Responses in Daphnia Magna. *PLoS One* **2014**, *9*, e92771.
- (15) Wiklund, A. K. E.; Breitholtz, M.; Bengtsson, B. E.; Adolfsson-Erici, M. Sucralose - an Ecotoxicological Challenger? *Chemosphere* **2012**, *86*, 50–55.
- (16) Labare, M. P.; Alexander, M. Microbial Cometabolism of Sucralose, a Chlorinated Disaccharide, in Environmental-Samples. *Appl. Microbiol. Biotechnol.* **1994**, *42*, 173–178.
- (17) Schiffman, S. S.; Rother, K. I. Sucralose, a Synthetic Organochlorine Sweetener: Overview of Biological Issues. *J. Toxicol. Environ. Health, Part B* **2013**, *16*, 399–451.
- (18) Schiffman, S. S.; Abou-Donia, M. B. Sucralose Revisited: Rebuttal of Two Papers About Splenda Safety. *Regul. Toxicol. Pharmacol.* **2012**, *63*, 505–508.
- (19) Han, X.-L.; Mei, P.; Liu, Y.; Xiao, Q.; Jiang, F.-L.; Li, R. Binding Interaction of Quinclorac with Bovine Serum Albumin: A Biophysical Study. *Spectrochim. Acta, Part A* **2009**, *74*, 781–787.
- (20) Erickson, A.; Deibel, R. H. Production and Heat-Stability of Staphylococcal Nuclease. *Appl. Microbiol.* **1973**, *25*, 332–336.
- (21) Tang, J.; Zhou, R.; Shi, X.; Kang, M.; Wang, H.; Chen, H. Two Thermostable Nucleases Coexisted in Staphylococcus Aureus: Evidence from Mutagenesis and in Vitro Expression. *FEMS Microbiol. Lett.* **2008**, *284*, 176–183.
- (22) Bucci, E.; Steiner, R. F. Anisotropy Decay of Fluorescence as an Experimental Approach to Protein Dynamics. *Biophys. Chem.* **1988**, *30*, 199–224.
- (23) Lee, J. C.; Timasheff, S. N. The Stabilization of Proteins by Sucrose. *J. Biol. Chem.* **1981**, *256*, 7193–7201.
- (24) Kwon, O. H.; Yoo, T. H.; Othon, C. M.; Van Deventer, J. A.; Tirrell, D. A.; Zewail, A. H. Hydration Dynamics at Fluorinated Protein Surfaces. *Proc. Natl. Acad. Sci. U. S. A.* **2010**, *107*, 17101–17106.
- (25) Debye, P. J. W. *Polar Molecules*; The Chemical Catalog Company, Inc.: New York, 1929.
- (26) Mathlouthi, M.; Reiser, P. *Sucrose: Properties and Applications*; Blackie Academic & Professional: London, 1995.
- (27) Swiergiel, J.; Bouteiller, L.; Jadzyn, J. Compliance of the Stokes-Einstein Model and Breakdown of the Stokes-Einstein-Debye Model for a Urea-Based Supramolecular Polymer of High Viscosity. *Soft Matter* **2014**, *10*, 8457–8463.
- (28) Miyake, Y.; Hidemori, T.; Akai, N.; Kawai, A.; Shibuya, K.; Koguchi, S.; Kitazume, T. Epr Study of Rotational Diffusion in Viscous Ionic Liquids: Analysis by a Fractional Stokes-Einstein-Debye Law. *Chem. Lett.* **2009**, *38*, 124–125.
- (29) Swiergiel, J.; Jadzyn, J. Fractional Stokes-Einstein-Debye Relation and Orientational Entropy Effects in Strongly Hydrogen-Bonded Liquid Amides. *Phys. Chem. Chem. Phys.* **2011**, *13*, 3911–3916.
- (30) Turton, D. A.; Wynne, K. Stokes-Einstein-Debye Failure in Molecular Orientational Diffusion: Exception or Rule? *J. Phys. Chem. B* **2014**, *118*, 4600–4604.

(31) Harris, K. R. The Fractional Stokes-Einstein Equation: Application to Lennard-Jones, Molecular, and Ionic Liquids. *J. Chem. Phys.* **2009**, *131*, 054503.

(32) Richert, R. Heterogeneous Dynamics in Liquids: Fluctuations in Space and Time. *J. Phys.: Condens. Matter* **2002**, *14*, R703–R738.

(33) Bennion, B. J.; Daggett, V. The Molecular Basis for the Chemical Denaturation of Proteins by Urea. *Proc. Natl. Acad. Sci. U. S. A.* **2003**, *100*, 5142–5147.

(34) Shortle, D.; Meeker, A. K. Mutant Forms of Staphylococcal Nuclease with Altered Patterns of Guanidine Hydrochloride and Urea Denaturation. *Proteins: Struct., Funct., Genet.* **1986**, *1*, 81–89.

(35) Byrne, M. P.; Manuel, R. L.; Lowe, L. G.; Stites, W. E. Energetic Contribution of Side-Chain Hydrogen-Bonding to the Stability of Staphylococcal Nuclease. *Biochemistry* **1995**, *34*, 13949–13960.

(36) Swindells, J. F.; United States National Bureau of Standards. *Viscosities of Sucrose Solutions at Various Temperatures: Tables of Recalculated Values*; The Supt. of Docs., U.S. G.P.O.: Washington, DC, 1958.